Structural characterization of phosphatidylcholines using 193 nm ultraviolet photodissociation mass spectrometry

Dustin R. Klein, Jennifer S. Brodbelt

Department of Chemistry

The University of Texas at Austin

Austin, TX 78712, USA

Correspondence: jbrodbelt@cm.utexas.edu

Supporting Information: The contents of the supporting information include figures and tables showing the structures, masses and full mass spectra of all standard phosphatidylcholines (PCs), HCD and UVPD spectra of Na-cationized PC 16:0/18:1(9Z), HCD and UVPD spectra for PC 16:0/18:0, PC 16:0/18:1(9Z), PC 18:1(9Z)/16:0, and PC 16:0/18:1(9Z,12Z), HCD and UVPD spectra for all PCs identified in the polar bovine liver extract, full mass spectra and zoomed in UVPD mass spectra of samples containing varying molar ratios of PC 18:1(9Z)/18:1(9Z) and PC 18:1(6Z)/18:1(6Z). All figures with HCD and UVPD spectra contain accompanying fragmentation maps.

Table S1. Structures of all standard PCs

Lipid Name	Structure	Molecular mass (Da)
1-palmitoyl-2-oleoyl-*sn*-glycero-3-phosphocholine [PC 16:0/18:1(9Z)]	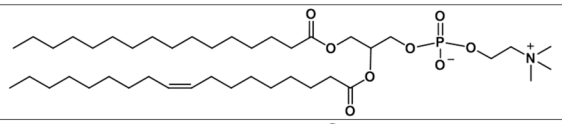	759.58
1,2-dioleoyl-*sn*-glycero-3-phosphocholine [PC 18:1(9Z)/18:1(9Z)]	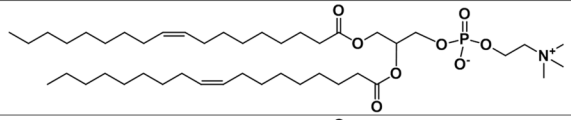	785.59
1,2-dipetroselenoyl-*sn*-glycero-3-phosphocholine [PC 18:1(6Z)/18:1(6Z)]	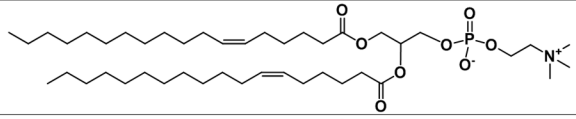	785.59
1,2-distearoyl-*sn*-glycero-3-phosphocholine [PC 18:0/18:0]	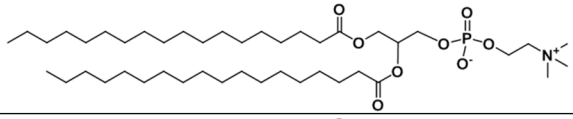	789.62
1-stearoyl-2-oleoyl-*sn*-glycero-3-phosphocholine [PC 18:0/18:1(9Z)]	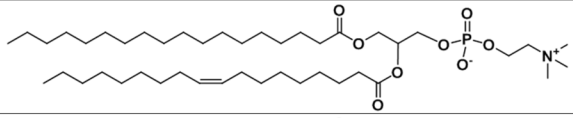	787.61
1-stearoyl-2-linoleoyl-*sn*-glycero-3-phosphocholine [PC 18:0/18:2(9Z,12Z)]	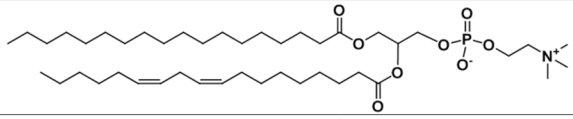	785.59
1-palmitoyl-2-stearoyl-*sn*-glycero-3-phosphocholine [PC 18:1(9Z)/16:0]	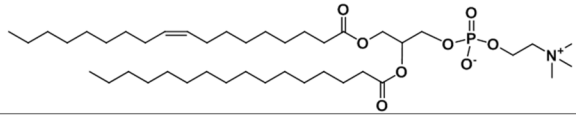	759.58

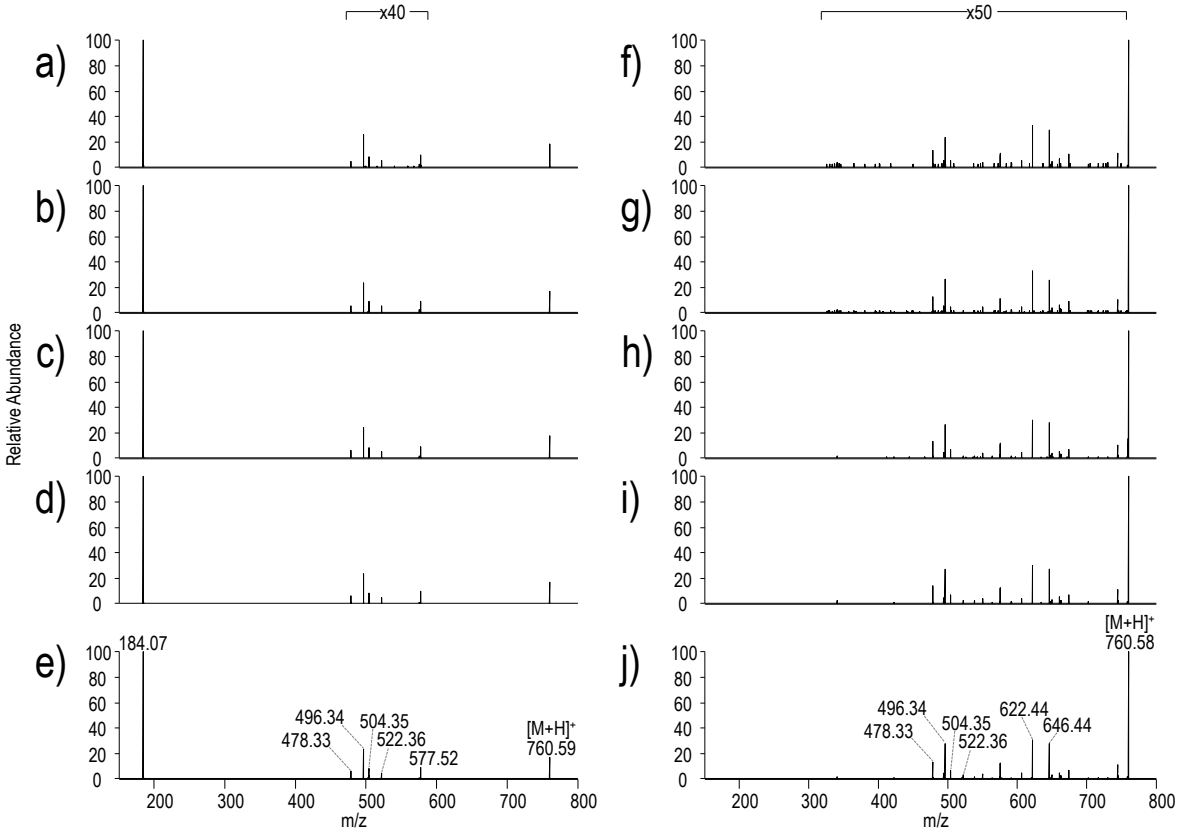

Figure S1. HCD mass spectra acquired for the ion of *m/z* 760.58 ($[M+H]^+$) from polar bovine liver extract with a) 1, b) 2, c) 5, d) 10 and e) 20 scans averaged. UVPD spectra acquired for the ion of *m/z* 760.58 ($[M+H]^+$) from polar bovine liver extract with f) 1, g) 2, h) 5, i) 10 and j) 20 scans averaged. Each scan contains 2 µscans.

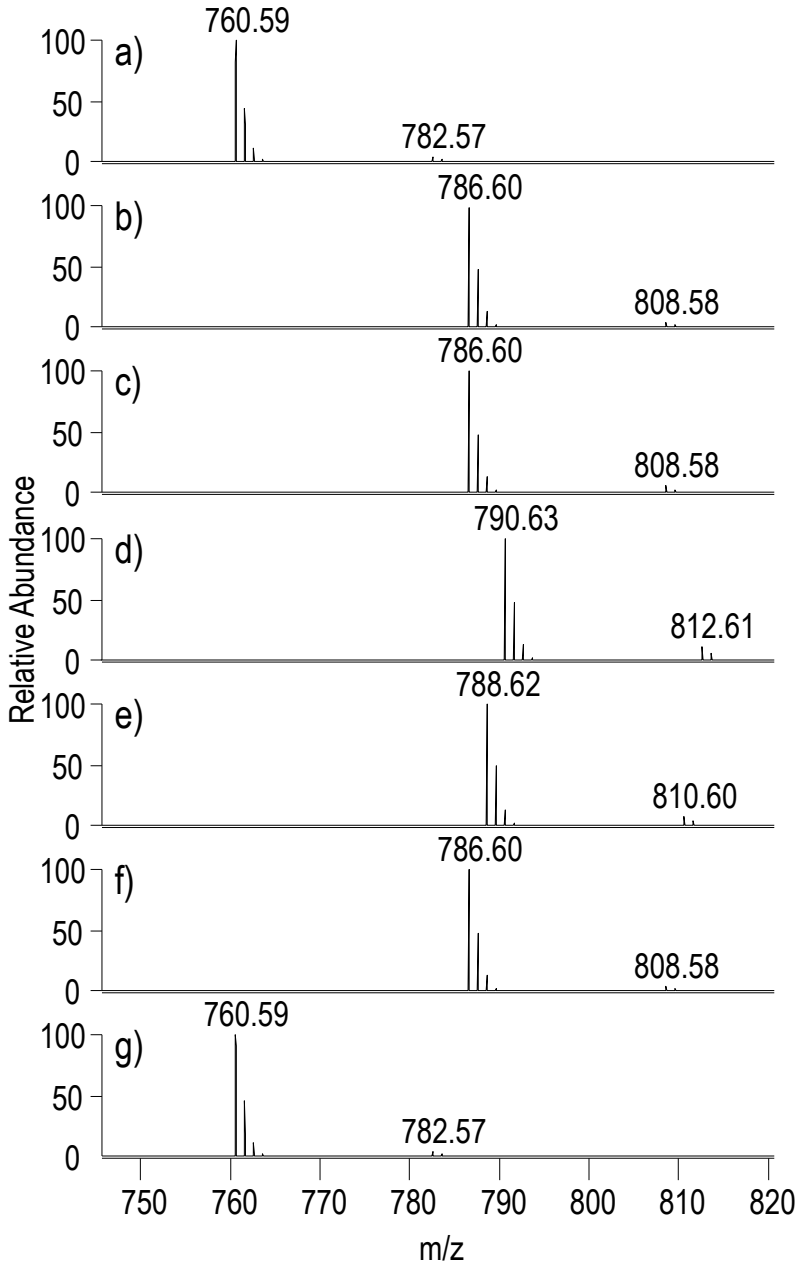

Figure S2. MS1 spectra of a) PC 16:0/18:1(9Z), b) PC 18:1(9Z)/18:1(9Z), c) PC 18:1(6Z)/18:1(6Z), d) PC 18:0/18:0, e) PC 18:0/18:1(9Z), f) PC 18:0/18:2(9Z,12Z), and g) PC18:1(9Z)/16:0

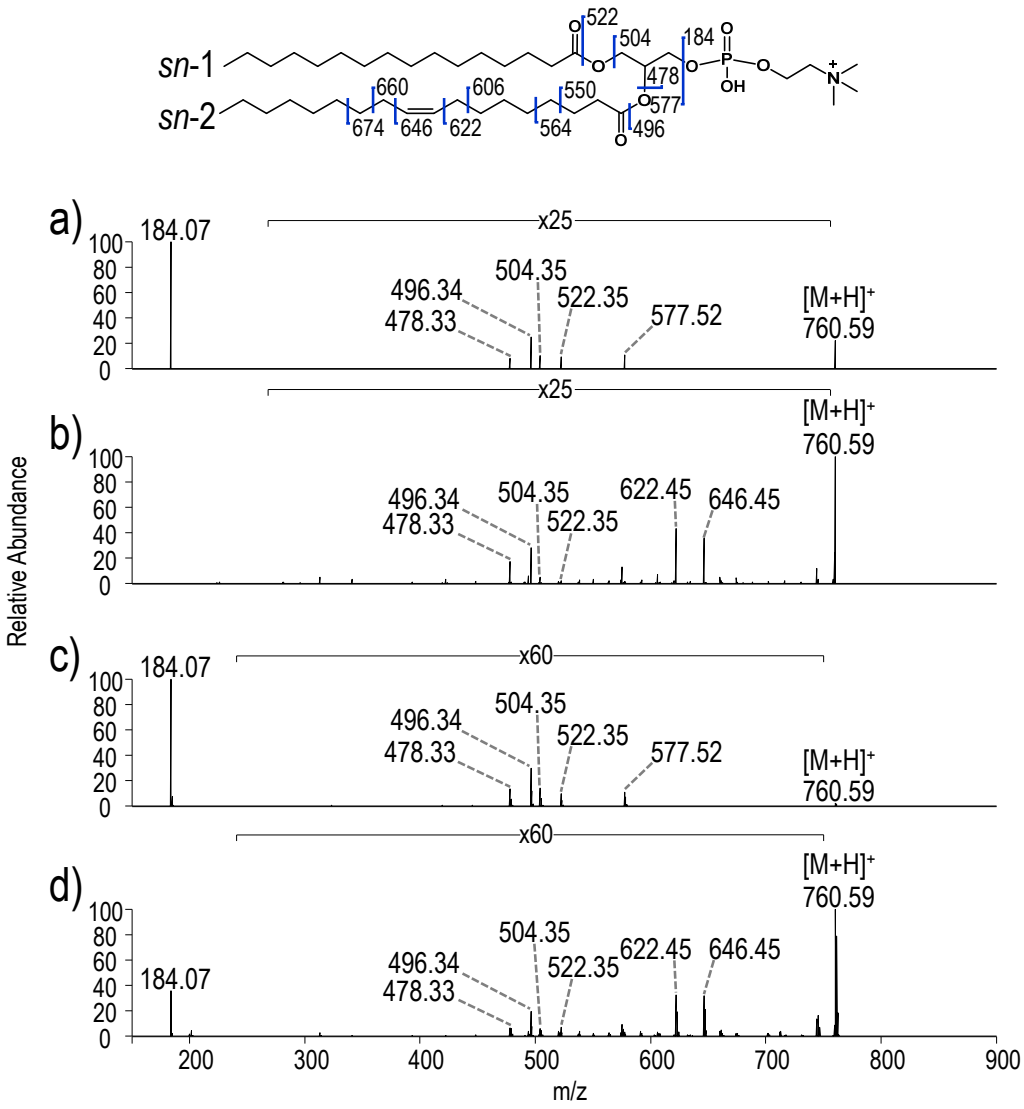

Figure S3. a) HCD (NCE 25) and b) UVPD (10 pulses, 6 mJ) of PC 16:0/18:1(9Z) ($[M+H]^+$, *m/z* 760.59) collected on the Orbitrap Fusion Lumos mass spectrometer. c) HCD (NCE 25) and b) UVPD (8 pulses, 5 mJ) of PC 16:0/18:1(9Z) collected on the Orbitrap Elite mass spectrometer.

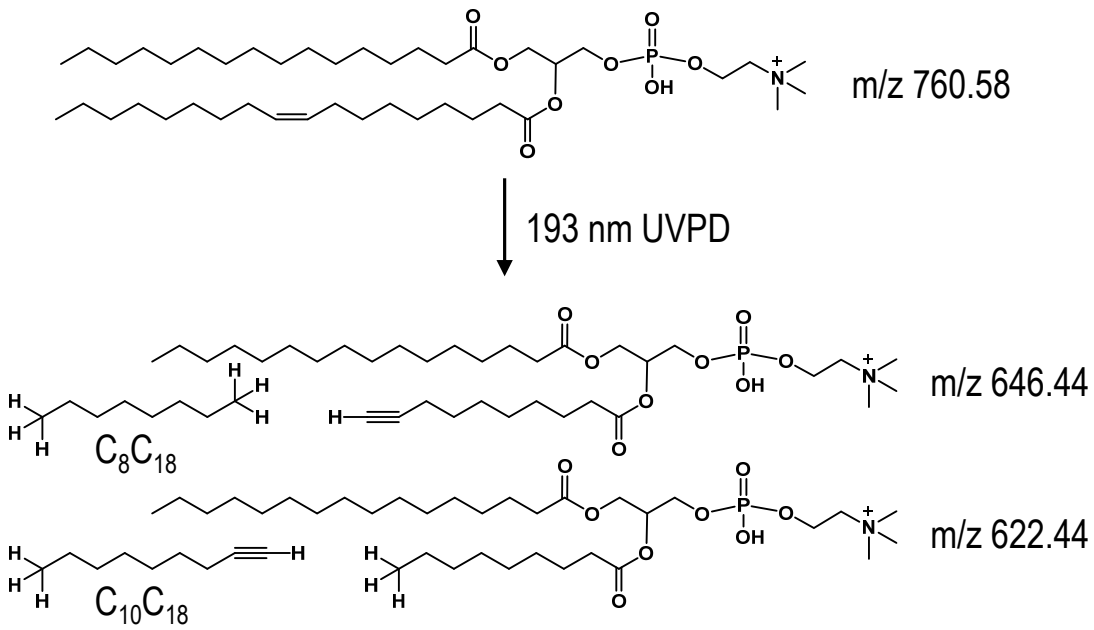

Figure S4. Proposed structures for diagnostic ions

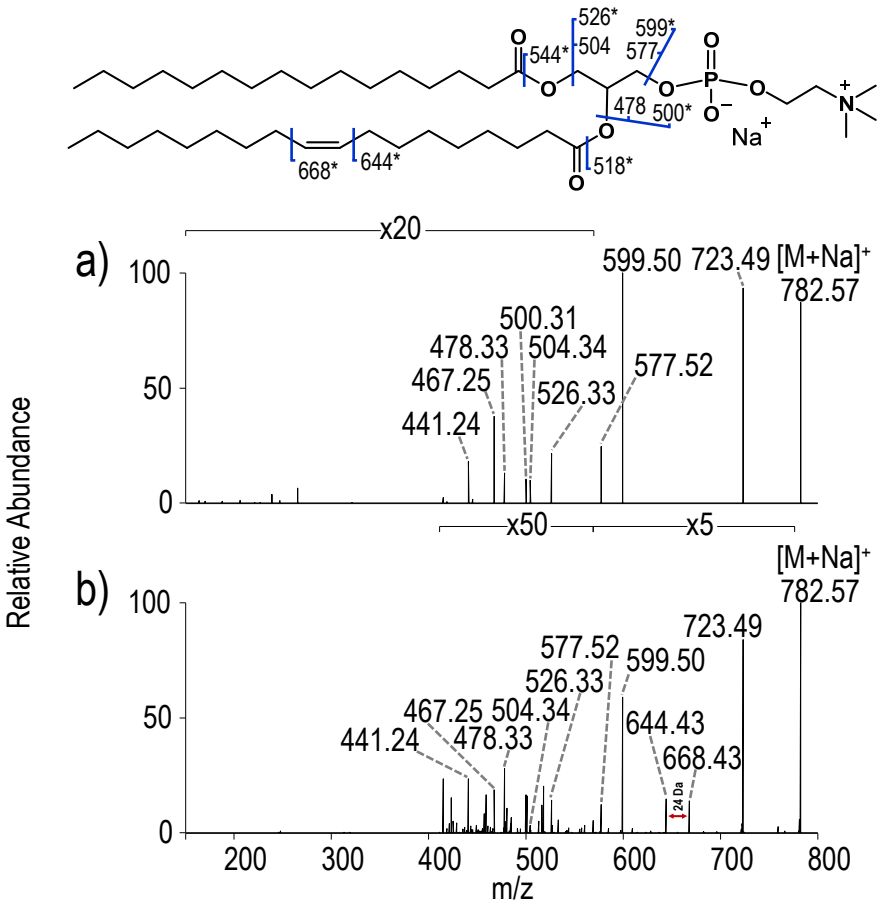

Figure S5. a) HCD (NCE 25) and b) UVPD (10 pulses, 6 mJ) of sodium-adducted PC 16:0/18:1(9Z) ($[M+Na]^+$, *m/z* 782.57)

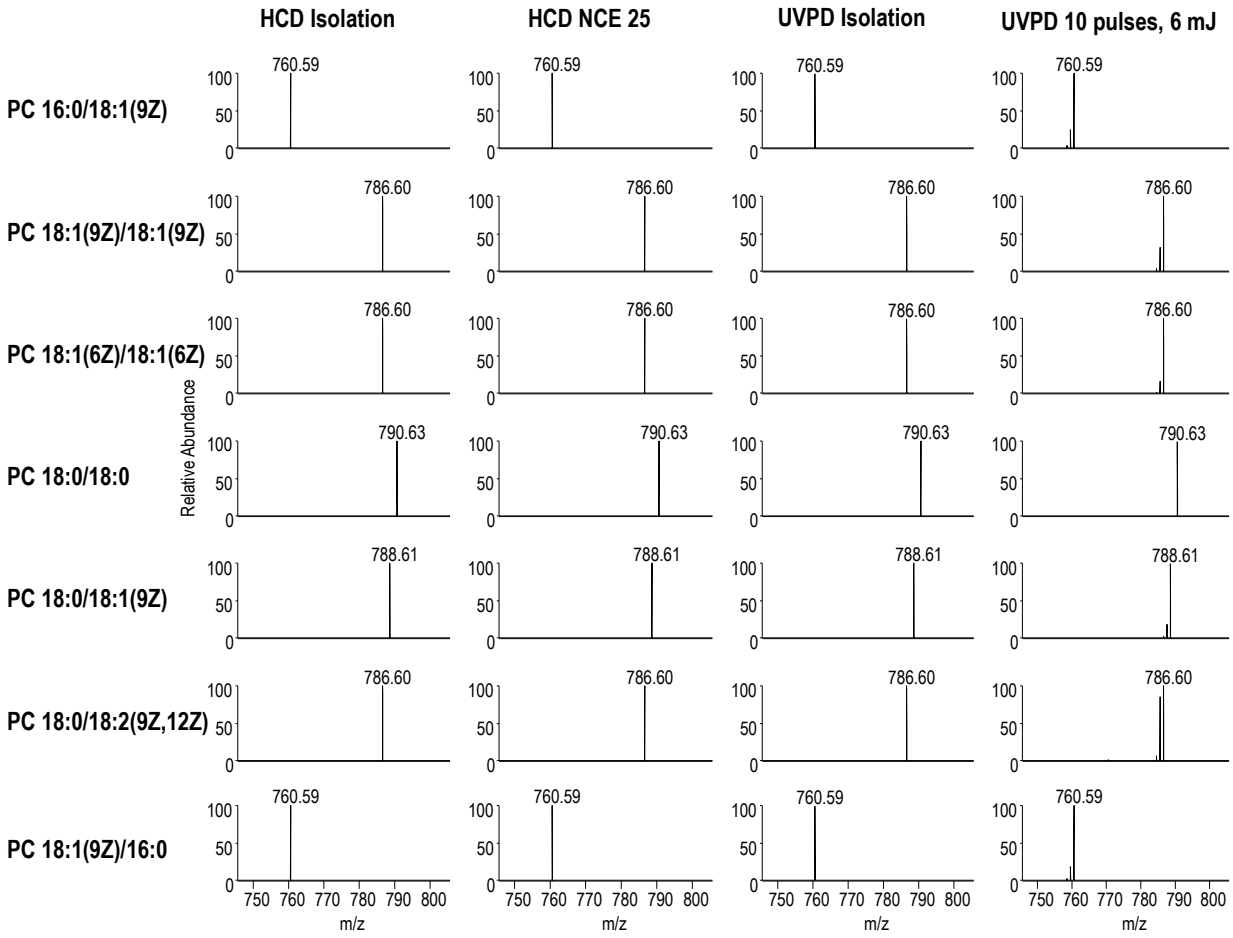

Figure S6. Expanded regions of mass spectra showing precursor isolation prior to HCD, HCD (NCE 25), precursor isolation prior to UVPD, and UVPD (10 pulses, 6 mJ) for PC 16:0/18:1(9Z), PC 18:1(9Z)/18:1(9Z), PC 18:1(6Z)/18:1(6Z), PC 18:0/18:0, PC 18:0/18:1(9Z), PC 18:0/18:2(9Z,12Z) and PC18:1(9Z)/16:0.

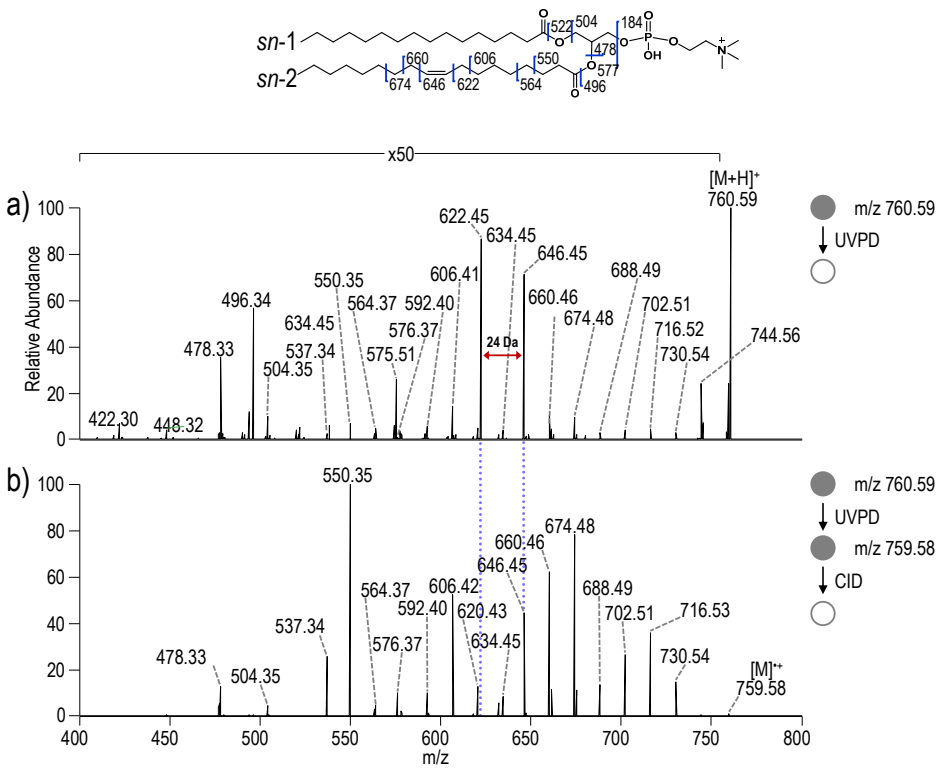

Figure S7. a) UVPD (10 pulses, 6 mJ) of PC 16:0/18:1(9Z) and b) UVPD-CID (10 pulses, 6 mJ-NCE 30) of PC 16:0/18:1(9Z). UVPD-CID is an MS3 event where UVPD is first performed on *m/z* 760.59 and then CID is subsequently performed on the hydrogen atom loss species of *m/z* 759.58.

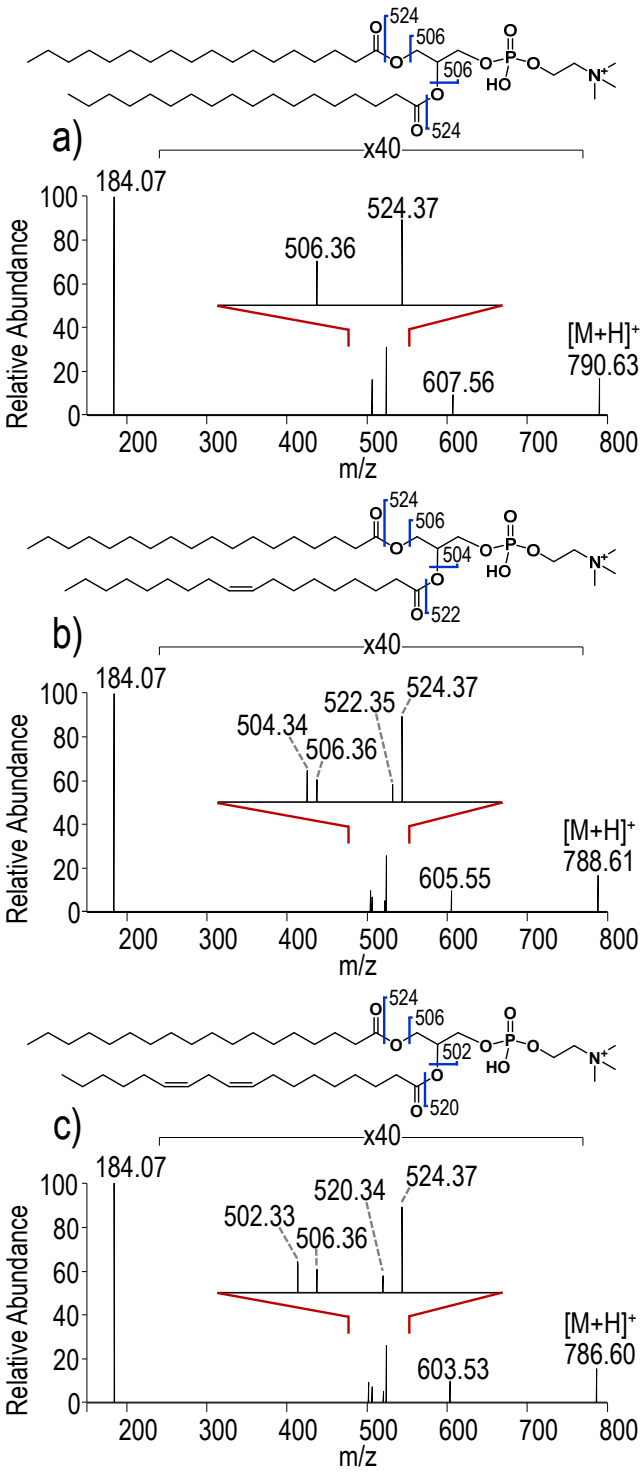

Figure S8. HCD (NCE 25) spectra of a) PC 18:0/18:0 ([M+H]$^+$, *m/z* 790.63), b) PC 18:0/18:1(9Z) ([M+H]$^+$, *m/z* 788.61), c) PC 18:0/18:2(9Z,12Z) ([M+H]$^+$, *m/z* 786.60).

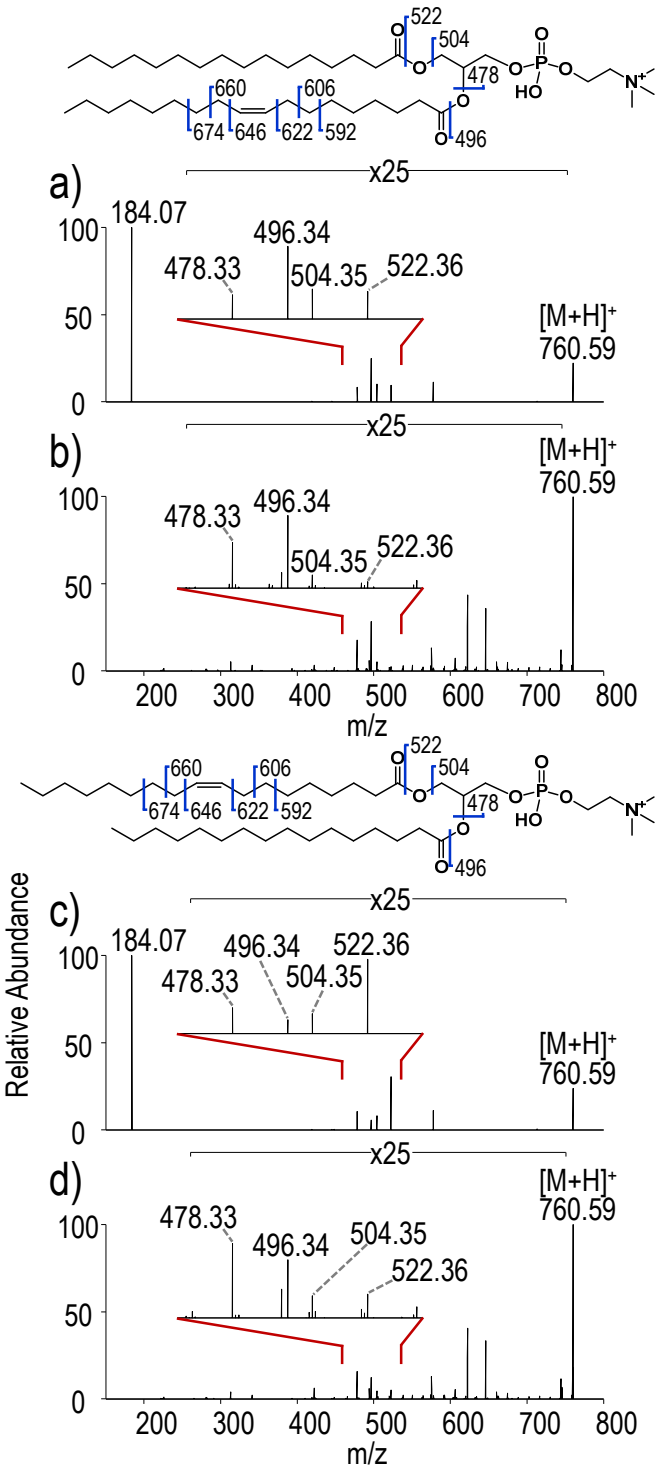

Figure S9. a) HCD (NCE 25) and b) UVPD (10 pulses, 6 mJ) of PC 16:0/18:1(9Z) ($[M+H]^+$, *m/z* 760.58). c) HCD (NCE 25) and d) UVPD (10 pulses, 6 mJ) of PC 18:1(9Z)/16:0 ($[M+H]^+$, *m/z* 760.58).

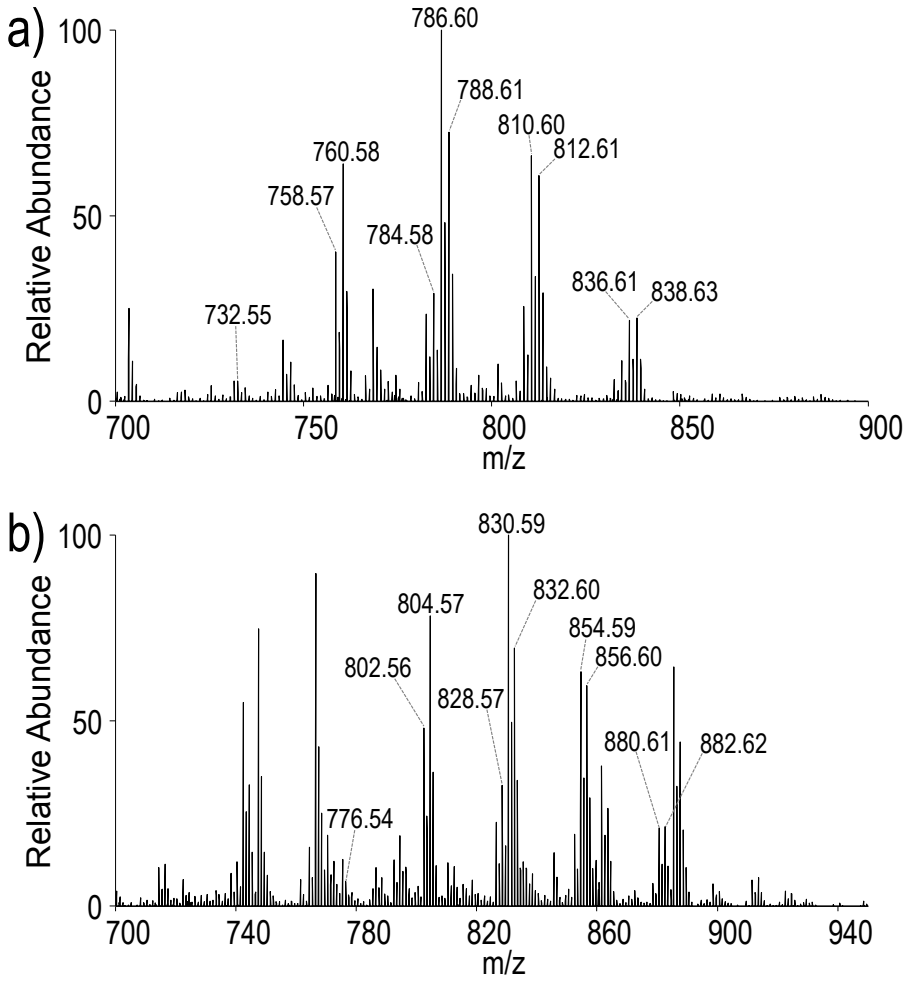

Figure S10. a) Positive mode and b) negative mode MS1 spectra of 10 µg/mL bovine liver extract in 50:50 ACN:H_2O with 30 mM ammonium formate.

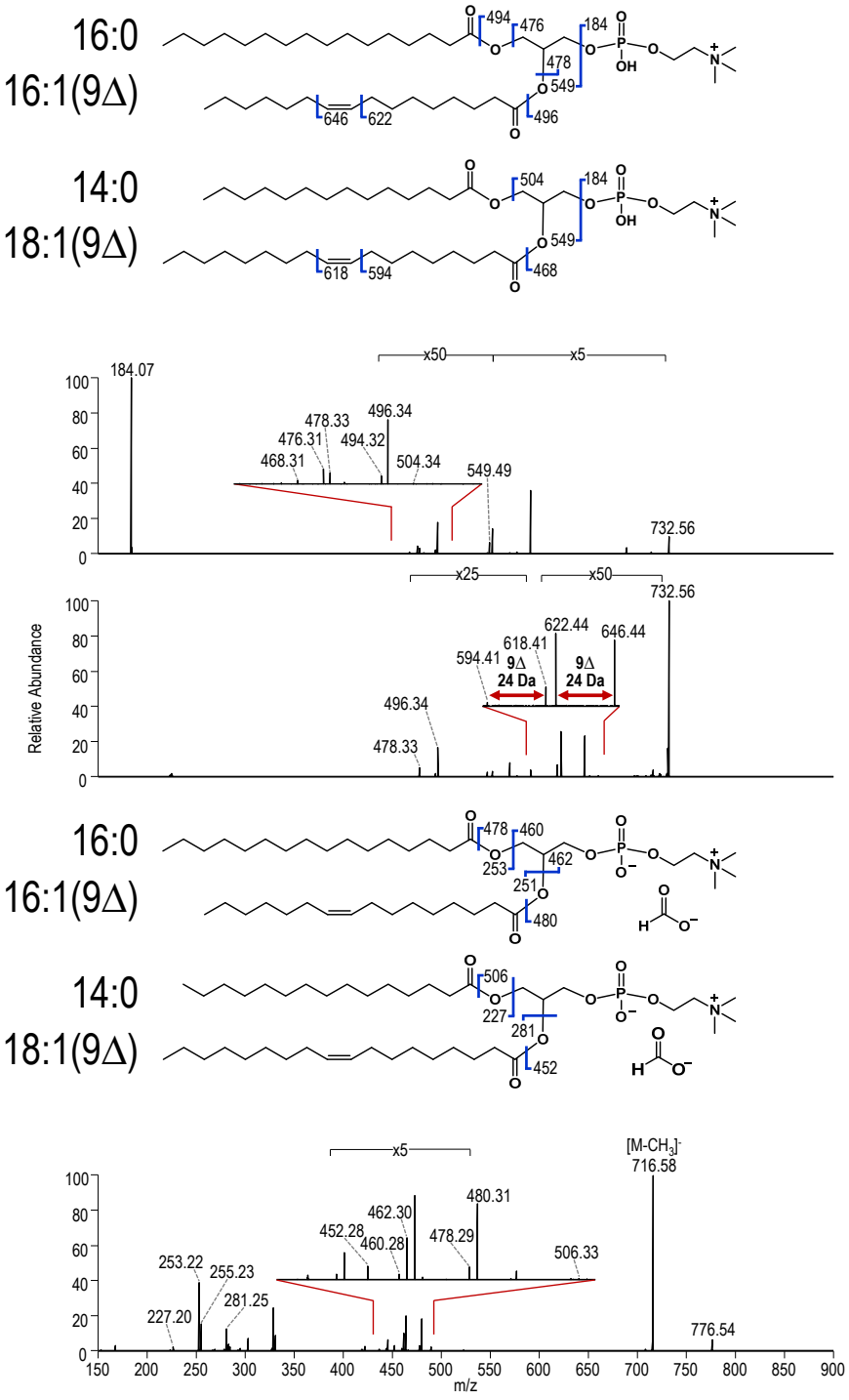

Figure S11. a) HCD and b) UVPD spectra of *m/z* 732.56 ($[M+H]^+$) and c) HCD spectrum of *m/z* 776.54 ($[M+COOH]^-$)

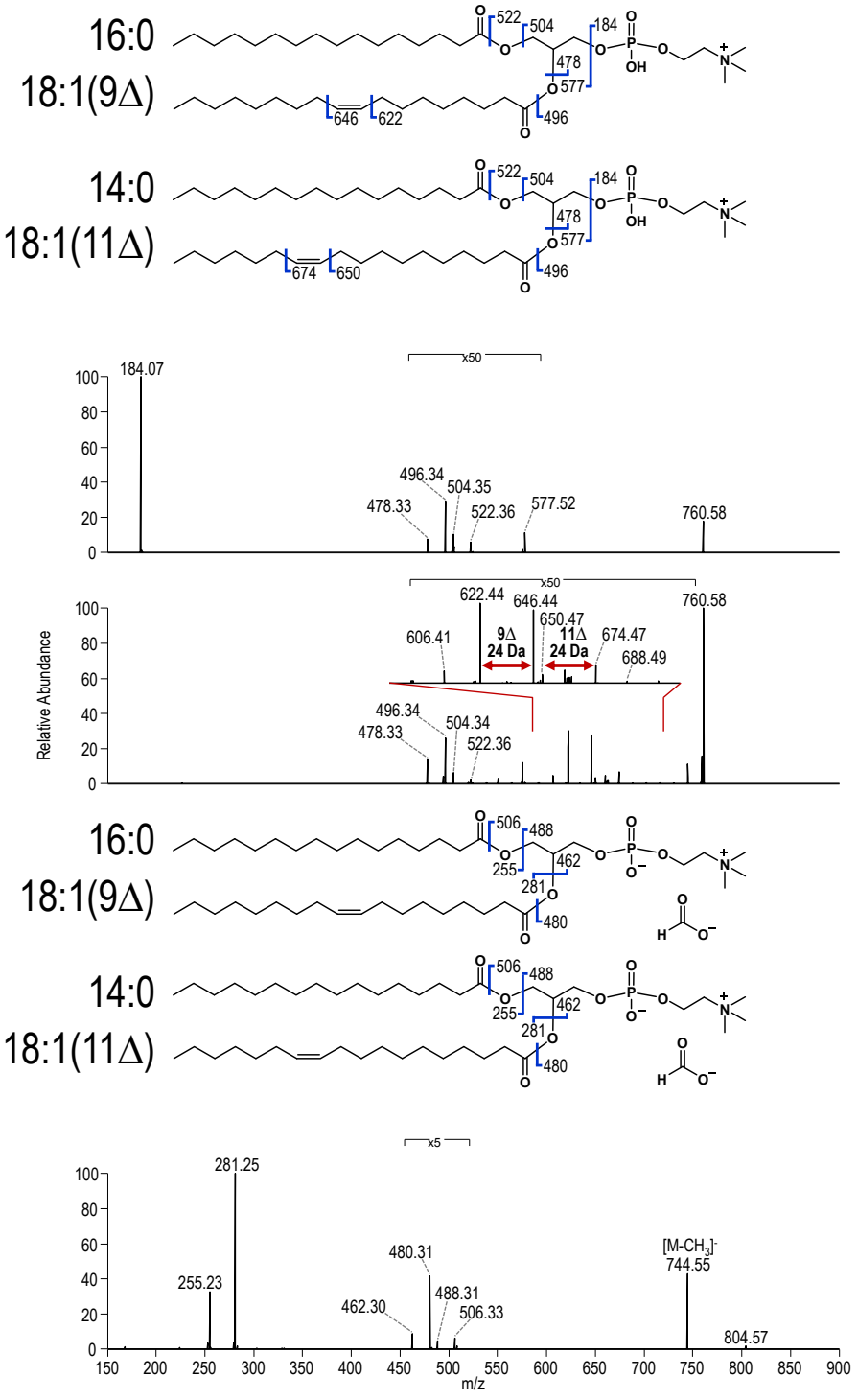

Figure S12. a) HCD and b) UVPD spectra of *m/z* 760.58 ($[M+H]^+$) and c) HCD spectrum of *m/z* 804.57 ($[M+COOH]^-$)

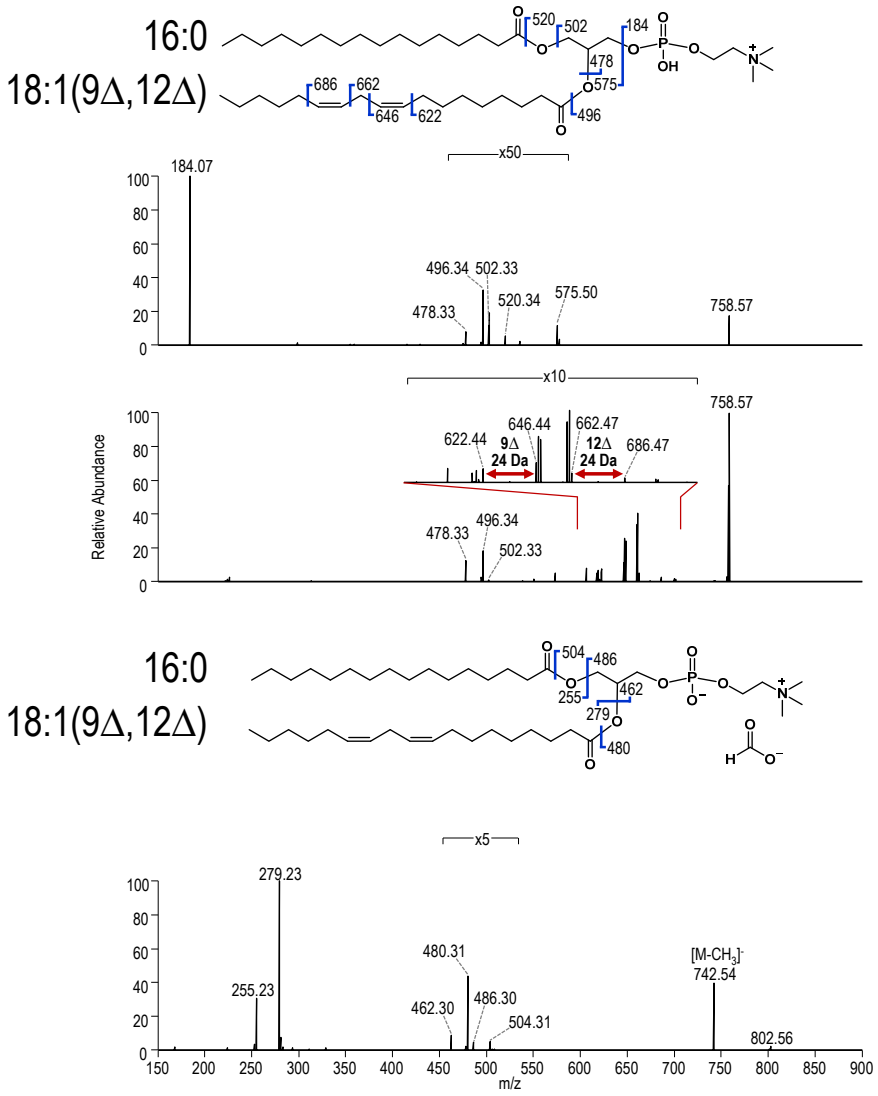

Figure S13. a) HCD and b) UVPD spectra of *m/z* 758.57 ($[M+H]^+$) and c) HCD spectrum of *m/z* 802.56 ($[M+COOH]^-$)

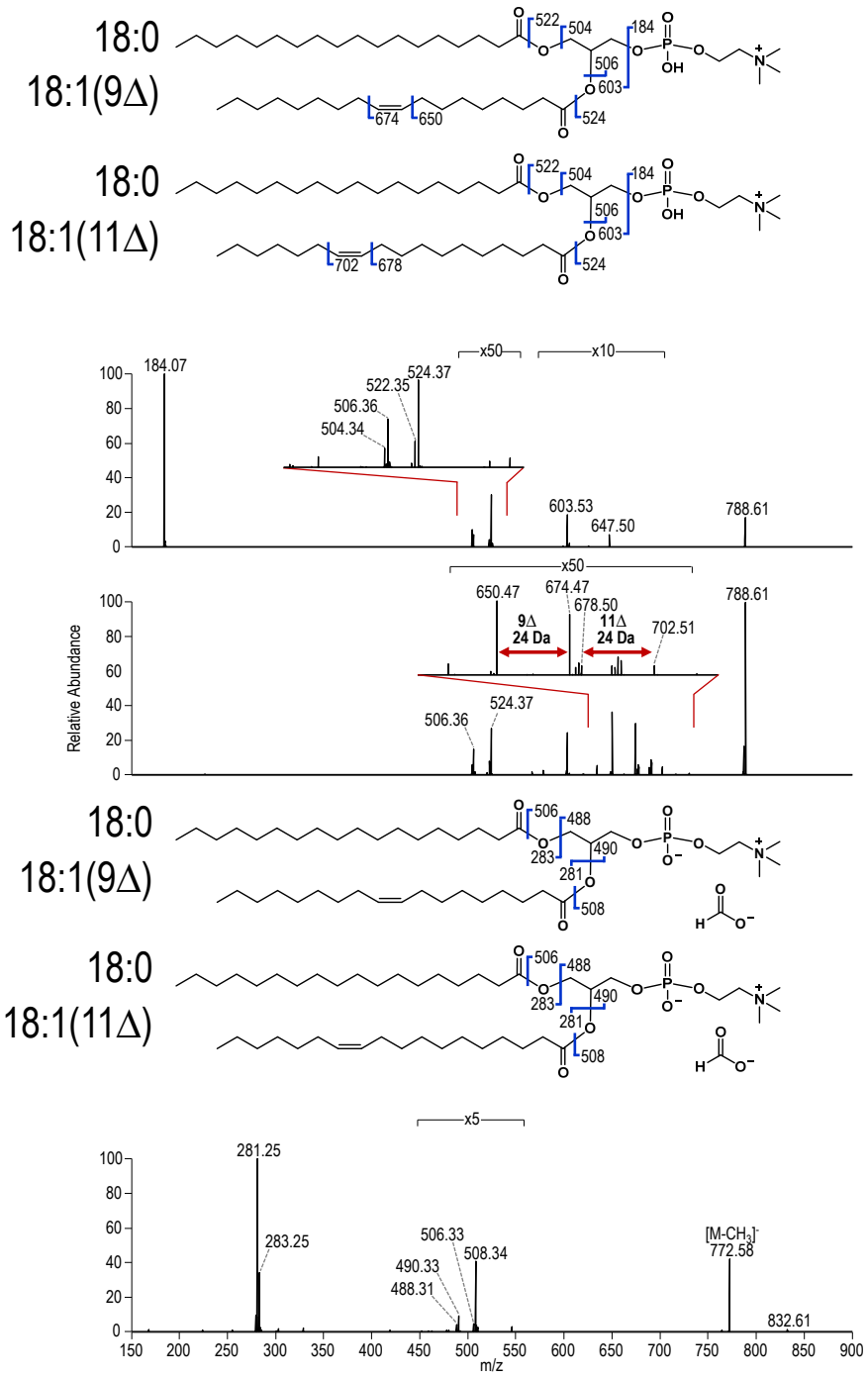

Figure S14. a) HCD and b) UVPD spectra of *m/z* 788.61 ($[M+H]^+$) and c) HCD spectrum of *m/z* 832.60 ($[M+COOH]^-$)

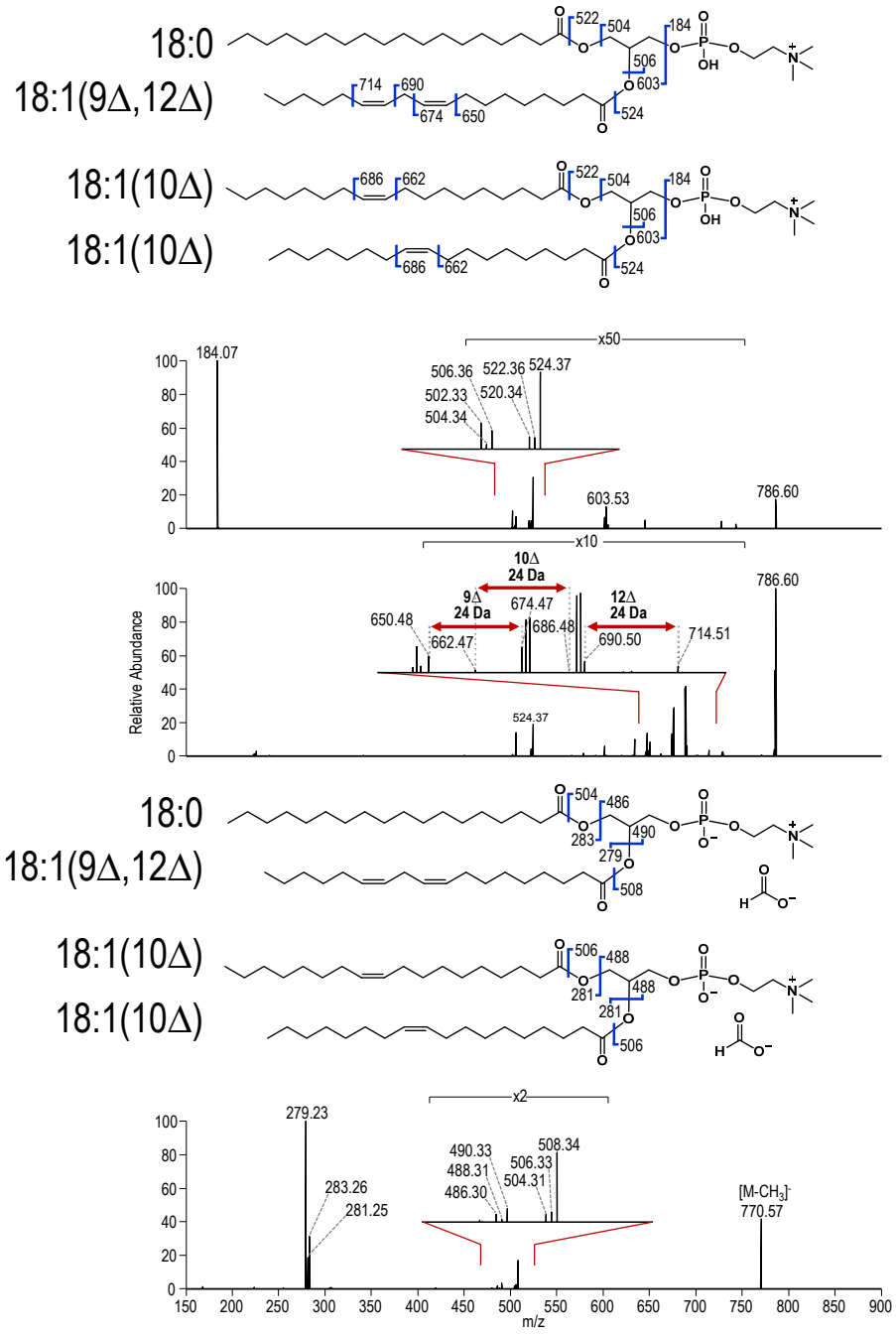

Figure S15. a) HCD and b) UVPD spectra of *m/z* 786.60 ($[M+H]^+$) and c) HCD spectrum of *m/z* 830.59 ($[M+COOH]^-$)

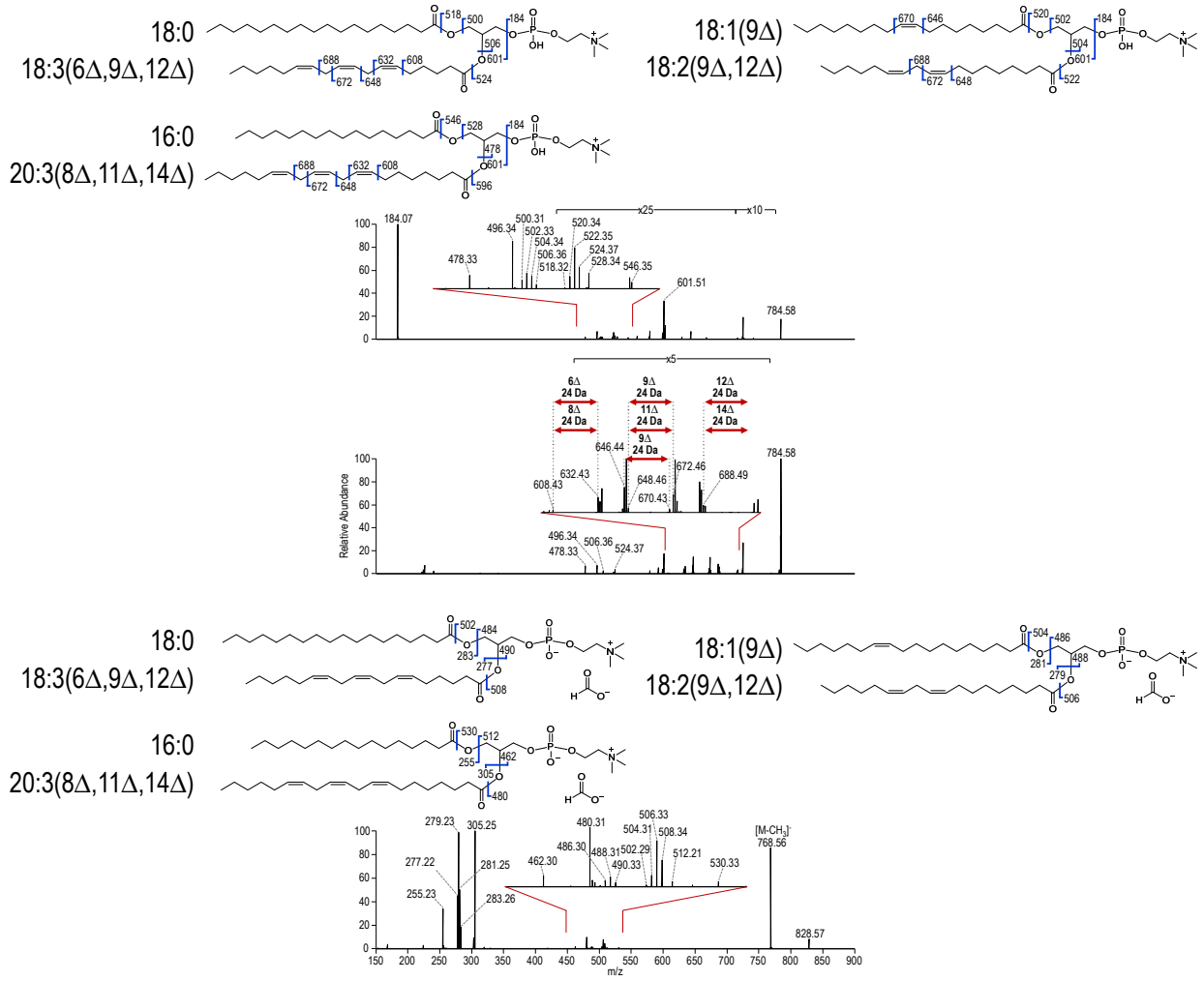

Figure S16. a) HCD and b) UVPD spectra of *m/z* 784.58 ($[M+H]^+$) and c) HCD spectrum of *m/z* 828.57 ($[M+COOH]^-$)

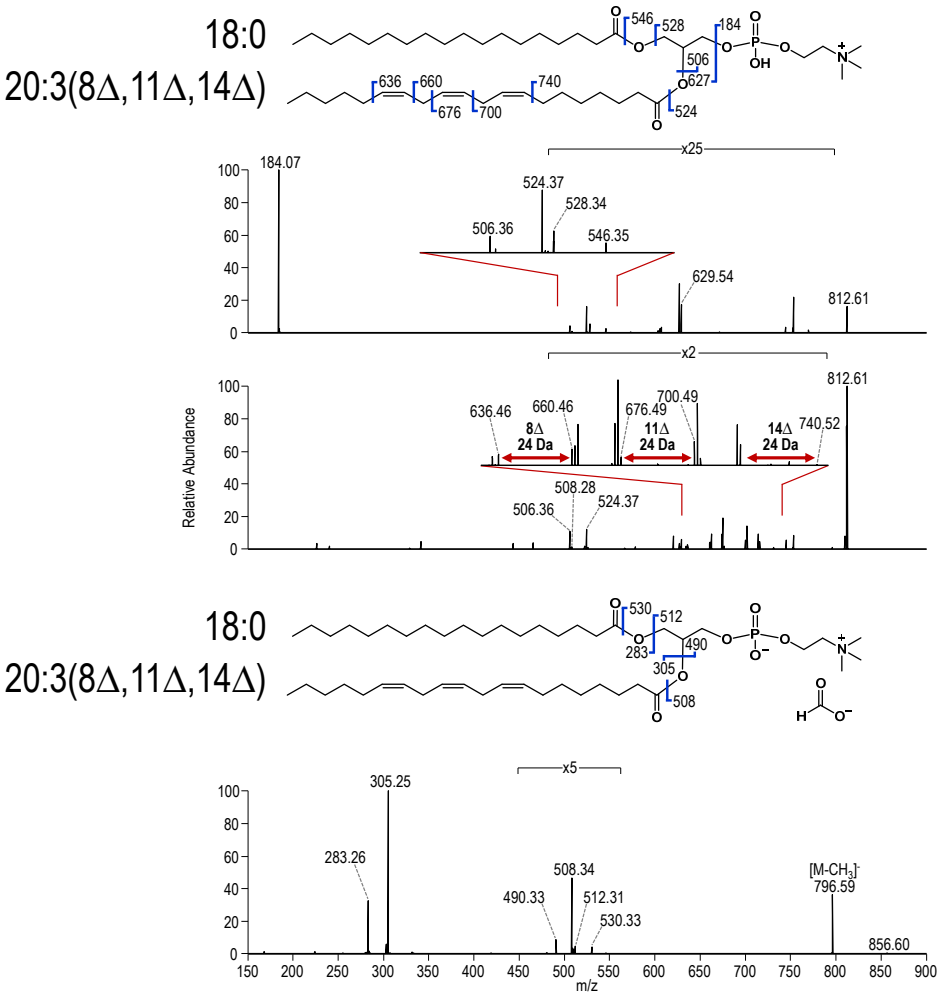

Figure S17. a) HCD and b) UVPD spectra of *m/z* 812.61 ($[M+H]^+$) and c) HCD spectrum of *m/z* 856.60 ($[M+COOH]^-$)

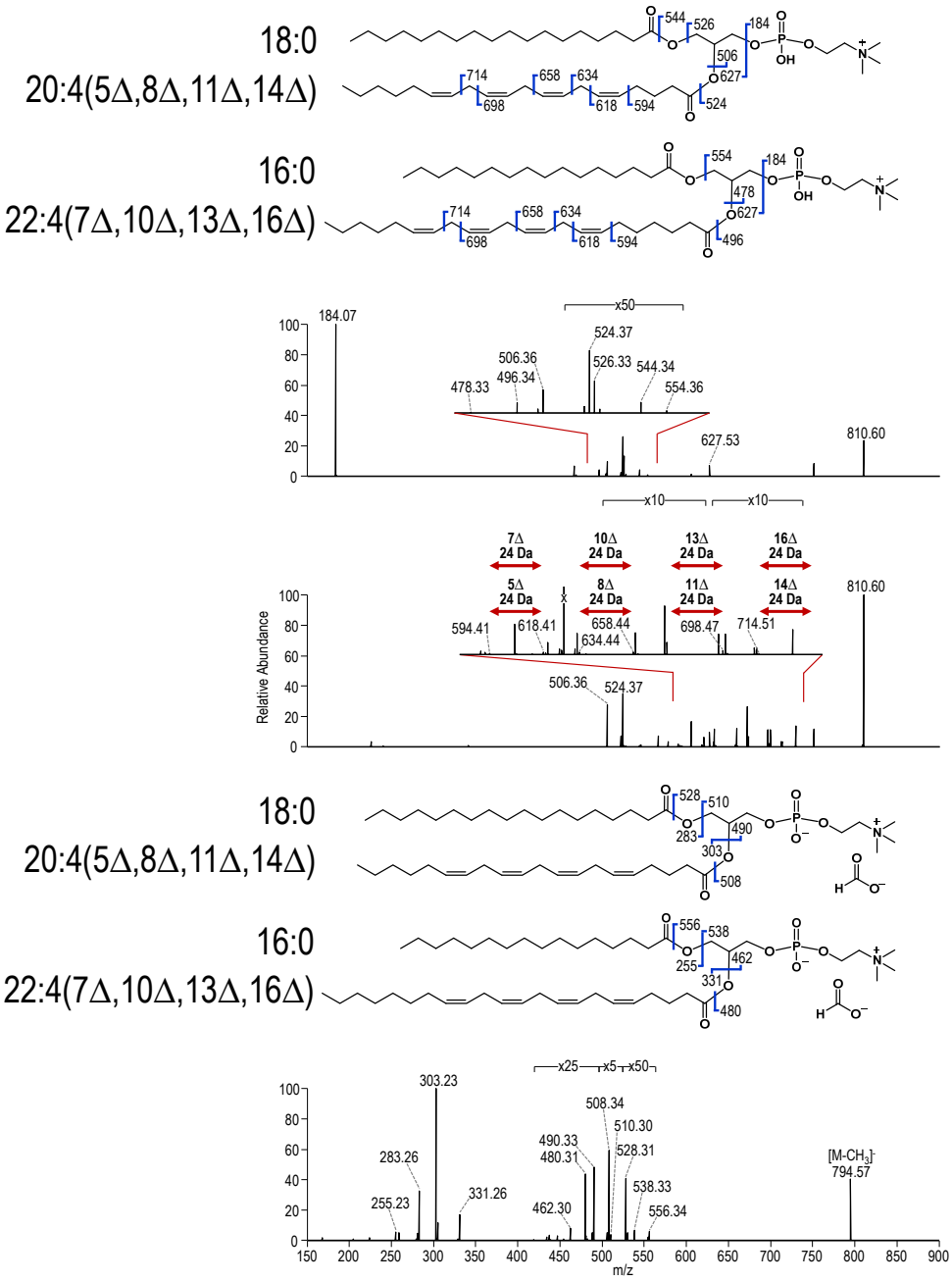

Figure S18. a) HCD and b) UVPD spectra of *m/z* 810.60 ($[M+H]^+$) and c) HCD spectrum of *m/z* 854.59 ($[M+COOH]^-$)

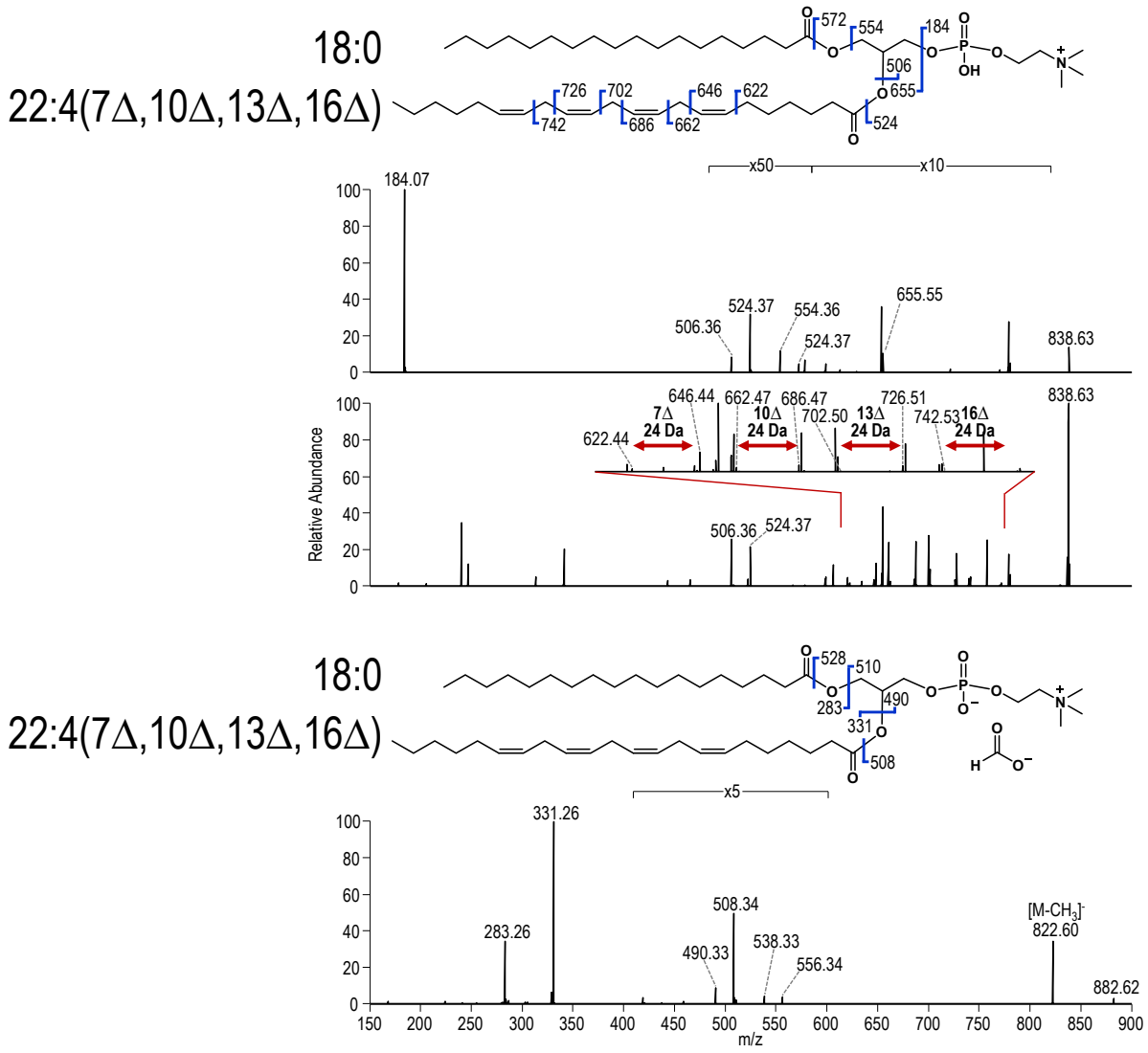

Figure S19. a) HCD and b) UVPD spectra of *m/z* 838.63 ($[M+H]^+$) and c) HCD spectrum of *m/z* 882.62 ($[M+COOH]^-$)

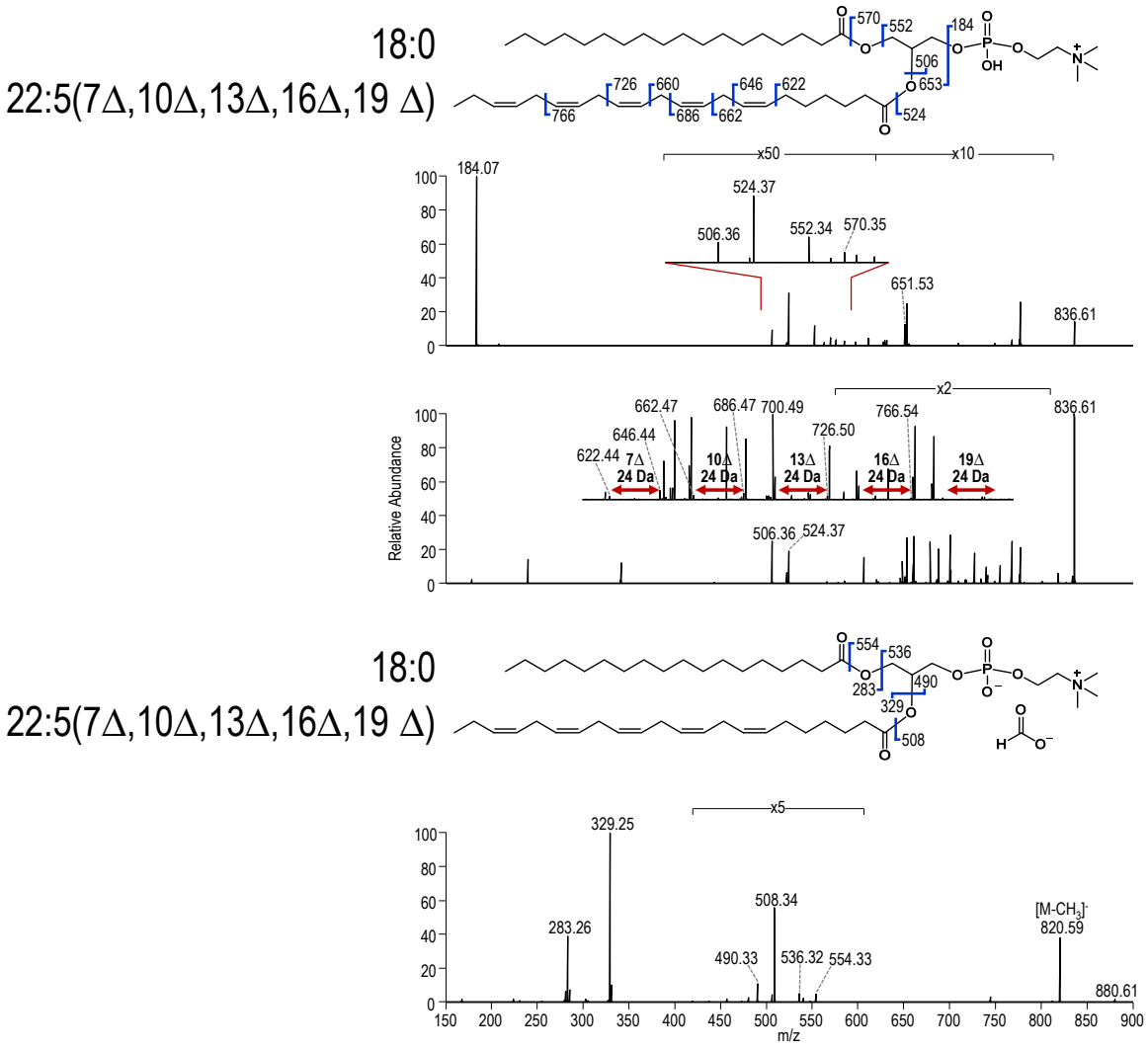

Figure S20. a) HCD and b) UVPD spectra of *m/z* 836.61 ($[M+H]^+$) and c) HCD spectrum of *m/z* 880.61 ($[M+COOH]^-$)

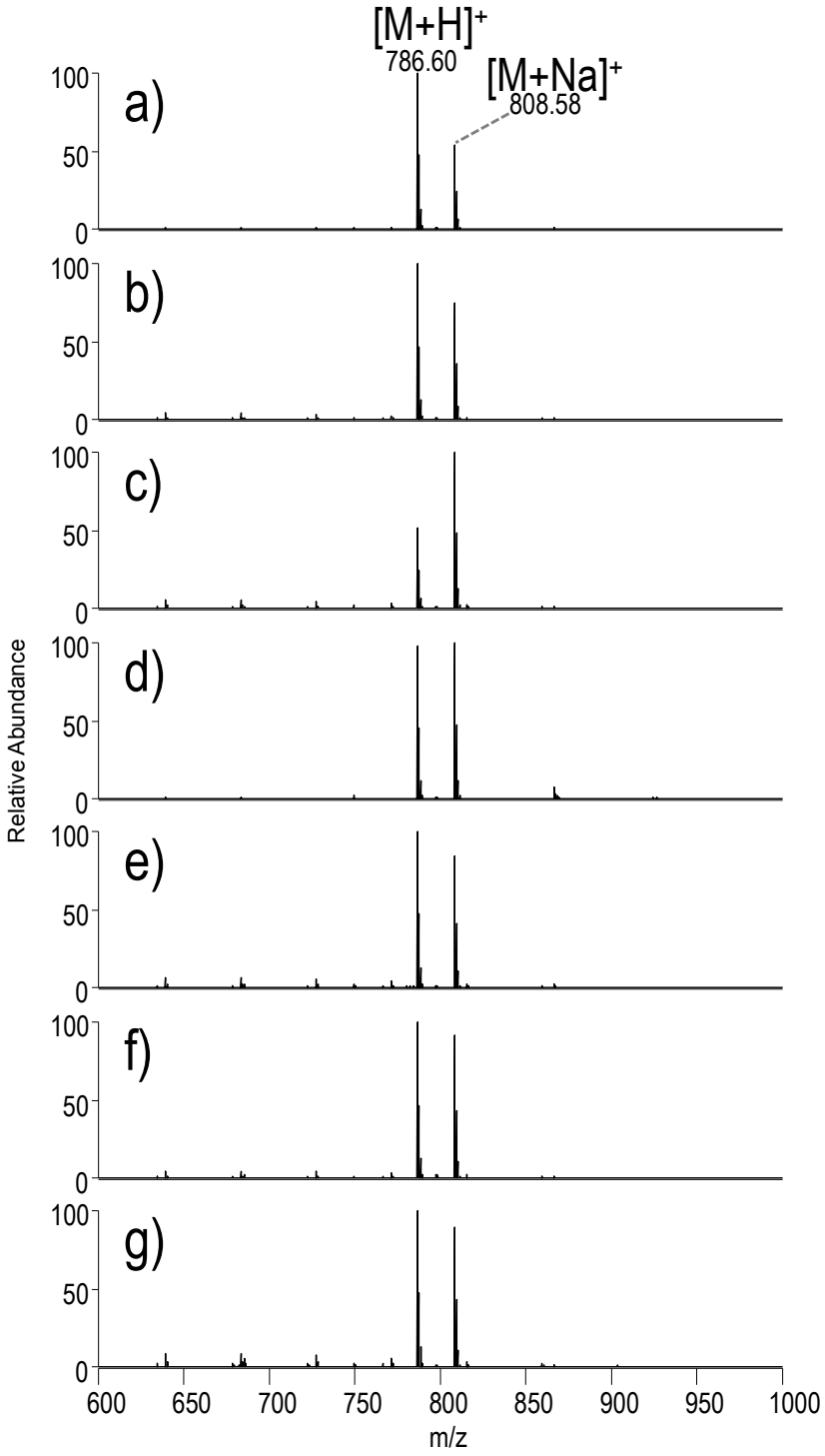

Figure S21. MS1 spectra of solutions containing different molar ratios of PC 18:1(9Z)/18:1(9Z) (1+, *m/z* 786.60) and PC 18:1(6Z)/18:1(6Z) (1+, *m/z* 786.60). a) 9:1, b) 7:3, c) 6:4, d) 5:5, e) 4:6, f) 3:7, g) 1:9. The total PC concentration for each solution is 10 uM. These samples were constituted in 50:50 MeOH:$CHCl_3$.

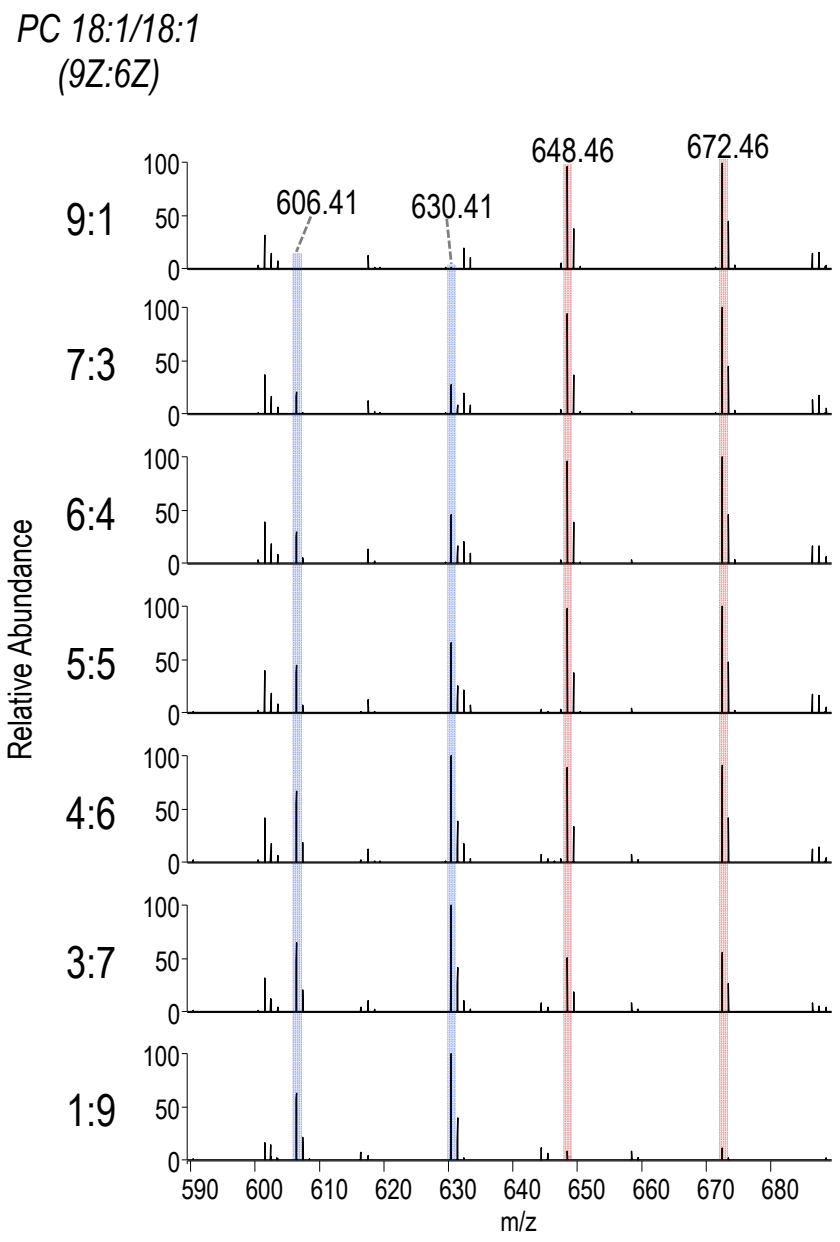

Figure S22. Expanded regions of the UVPD spectra for solutions containing various molar ratios of PC 18:1(9Z)/18:1(9Z) and PC 18:1(6Z)/18:1(6Z). These spectra show changes in the abundances of ions that are diagnostic of double bond position as the molar ratio of double bond isomers is varied.